2510 *J. Am. Chem. Soc.* **1992**, *114*, 2510–2520

Organometallic "Helicopters": Stereochemical Nonrigidity of μ_3-Arene/Olefin Triosmium Complexes in Solution and the Solid State

Mark A. Gallop, Brian F. G. Johnson, James Keeler, Jack Lewis,* Stephen J. Heyes, and Christopher M. Dobson

Contribution from the University Chemical Laboratory, Lensfield Road, Cambridge, CB2 1EW, U.K., and Inorganic Chemistry Laboratory, South Parks Road, Oxford, OX1 3QR, U.K.

Received October 11, 1989. Revised Manuscript Received October 23, 1991

Abstract: The nonrigidity of μ_3-arene/olefin triosmium complexes $[Os_3(CO)_8(\eta^2\text{-}CH_2CHR)(\mu_3{:}\eta^2{:}\eta^2{:}\eta^2\text{-}C_6H_6)]$, R = H, Me, Ph, ^{t}*Bu*, has been investigated through a series of one- and two-dimensional NMR experiments in solution, and five independent fluxional processes have been detected. $^{13}C\{^1H\}$ two-dimensional exchange spectroscopy clearly defines a 1,2 ring-hopping motion that permutes nuclei in the face-capping benzene ligands, while the π-bound olefins are fluxional through rotation about their metal–ligand axes and by a trigonal twist pathway that interchanges ligands in the $Os(CO)_2$(olefin) polytopes. These intramolecular rearrangements are designated "helicopter-like" behavior. Localized "turnstile" rotations also operate among the two tricarbonyl ligand sets. $^{13}C\{^1H\}$ cross-polarization magic angle spinning (CP/MAS) NMR experiments suggest that analogous processes may occur in the solid state.

Investigations of ligand mobility in metal cluster complexes have predominantly concerned the migration of carbonyl and hydride moieties with several general mechanisms having been recognized.[1] By comparison, stereodynamic processes associated with organic ligands in clusters have received rather scant attention, although the literature of mononuclear organometallic fluxionality is replete with mechanistic studies. For example, the nonrigidity of polyene and polyenyl ligands coordinated at one or two metal centers has been extensively treated.[2] Cluster complexes containing cyclic polyenes bonded at a single metal atom,[3] bridging one edge of a metal triangle[4] or capping a triangular face,[5] are also known to be fluxional, but the mechanistic aspects of these dynamic processes are frequently ill-defined.

We are currently developing the chemistry of triosmium carbonyl clusters containing benzene in a face-capping bonding mode, $(\mu_3{:}\eta^2{:}\eta^2{:}\eta^2\text{-}C_6H_6)$, where the nature of the C_6 ligand is best regarded within the limiting descriptions of a bond-localized μ_3-cyclohexatriene and a completely delocalized μ_3-arene.[6] Activation barriers to intramolecular exchange between inequivalent ring protons in these complexes are typically low, and the face-capping ligands are fluxional at ambient temperature. This paper reports on the stereochemical nonrigidity of the μ_3-benzene/π-alkene complexes $[Os_3(CO)_8(\eta^2\text{-}CH_2CHR)(\mu_3{:}\eta^2{:}\eta^2{:}\eta^2\text{-}C_6H_6)]$, R = H (**1**), Me (**2**), Ph (**3**), ^{t}*Bu* (**4**), whose syntheses and characterization are described in the preceding paper in this issue.[6a] A series of variable temperature one- and two-dimensional NMR experiments in solution reveals that intriguing fluxional processes are associated with both the benzene and olefin ligands of these compounds, while familiar exchange pathways permute ligands in the supporting carbonyl envelopes. Specifically, we demonstrate the power of two-dimensional exchange spectroscopy (EXSY) in unravelling mechanistic details of complex, multisite exchange processes and for providing underlying kinetic and activation parameters. Moreover, preliminary $^{13}C\{^1H\}$ cross-polarization magic angle spinning (CP/MAS) studies on complex **1** indicate that cluster nonrigidity persists in the lattice. Portions of this work have previously been communicated.[6c]

Results and Discussion

The acetonitrile ligand in the face-capping benzene cluster $[Os_3(CO)_8(NCMe)(\mu_3{:}\eta^2{:}\eta^2{:}\eta^2\text{-}C_6H_6)]$ is readily displaced by two-electron donors (e.g., CO, pyridine, phosphines, and olefins) to afford complexes that retain the μ_3-arene.[6a] Substitution by alkenes $CH_2{=}CHR$, R = H, Me, Ph, ^{t}*Bu*, occurs at an equatorial coordination site, and in the ground-state geometry the C–C vector of the π-bonded ligand lies approximately in the plane of the metal triangle. The molecular structure of the η^2-ethylene compound **1** is reproduced in Figure 1, with ^1H and $^{13}C\{^1H\}$ NMR spectroscopic data for complexes **1**–**4** collected in Table I. Note that the assignments of the ethylene proton pairs H_A/H_B and H_C/H_D were inverted in error in our original report.[6c]

^1H NMR Spectra of $[Os_3(CO)_8(\eta^2\text{-}CH_2CHR)(\mu_3{:}\eta^2{:}\eta^2{:}\eta^2\text{-}C_6H_6)]$. The temperature dependence of the ^1H NMR spectra of the π-olefin derivatives $[Os_3(CO)_8(\eta^2\text{-}CH_2CHR)(\mu_3{:}\eta^2{:}\eta^2{:}\eta^2\text{-}C_6H_6)]$, R = H (**1**), Me (**2**), Ph (**3**), ^{t}*Bu* (**4**), has been examined and in every case limiting slow-exchange spectra can be obtained by ca. 180 K. Variable temperature spectra for complexes **1** and **2** are

---

* Address correspondence to this author at University Chemical Laboratory.

(1) (a) Johnson, B. F. G.; Benfield, R. E. In *Transition Metal Clusters*; Johnson, B. F. G., Ed.; John Wiley and Sons: Chichester, 1980. (b) Band, E.; Muetterties, E. L. *Chem. Rev.* **1978**, *78*, 639. (c) Evans, J. *Adv. Organomet. Chem.* **1977**, *16*, 319.

(2) (a) Mann, B. E. *Chem. Soc. Rev.* **1986**, *15*, 167 and references therein. (b) Mann, B. E. In *Comprehensive Organometallic Chemistry*; Wilkinson, G., Stone, F. G. A., Abel, E. W., Eds.; Pergamon: Oxford, 1981. (c) Cotton, F. A. In *Dynamic Nuclear Magnetic Resonance Spectroscopy*; Jackman, L. M., Cotton, F. A., Eds.; Academic Press: New York, 1975.

(3) Bau, R.; Burt, J. C.; Knox, S. A. R.; Laine, R. M.; Phillips, R. P.; Stone, F. G. A. *J. Chem. Soc., Chem. Commun.* **1973**, 726. (b) Whitesides, T. H.; Budnik, R. A. *J. Chem. Soc., Chem. Commun.* **1974**, 302. (c) Gancarz, R. A.; Baum, M. W.; Hunter, G.; Mislow, K. *Organometallics* **1986**, *5*, 2327. (d) Bryan, E. G.; Johnson, B. F. G.; Lewis, J. *J. Chem. Soc., Dalton Trans.* **1977**, 144. (e) Tachikawa, M.; Richter, S. I.; Shapley, J. R. *J. Organomet. Chem.* **1977**, *128*, C9. (f) Evans, J.; McNulty, G. S. *J. Chem. Soc., Dalton Trans.* **1984**, 79.

(4) (a) Bennett, M. J.; Cotton, F. A.; Legzdins, P. *J. Am. Chem. Soc.* **1967**, *89*, 6797. (b) Cotton, F. A.; Davison, A.; Musco, A. *J. Am. Chem. Soc.* **1967**, *89*, 6795. (c) Lyerla, J. R.; Fyfe, C. A.; Yannoni, C. S. *J. Am. Chem. Soc.* **1979**, *101*, 1351. (d) Bau, R.; Chou, B. C.-K.; Knox, S. A. R.; Riera, V.; Stone, F. G. A. *J. Organomet. Chem.* **1974**, *82*, C43. (e) Humphries, A. P.; Knox, S. A. R. *J. Chem. Soc., Dalton Trans.* **1978**, 1523. (f) Howard, J. A. K.; Knox, S. A. R.; Riera, V.; Stone, F. G. A.; Woodward, P. *J. Chem. Soc., Chem. Commun.* **1974**, 452. (g) Howard, J. A. K.; Knox, S. A. R.; Stone, F. G. A.; Szary, A. C.; Woodward, P. *J. Chem. Soc., Chem. Commun.* **1974**, 788. (h) Knox, S. A. R.; Stone, F. G. A. *Acc. Chem. Res.* **1974**, *7*, 321.

(5) (a) Fischer, E. O.; Mills, O. S.; Paulus, E. F.; Wawersik, H. *J. Chem. Soc., Chem. Commun.* **1967**, 643. (b) Mills, O. S.; Paulus, E. F. *J. Organomet. Chem.* **1968**, *11*, 587. (c) Humphries, A. P.; Knox, S. A. R. *J. Chem. Soc., Dalton Trans.* **1978**, 1523. (d) Howard, J. A. K.; Kennedy, F. G.; Knox, S. A. R. *J. Chem. Soc., Chem. Commun.* **1979**, 839. (e) Davidson, J. L.; Green, M.; Stone, F. G. A.; Welch, A. J. *J. Am. Chem. Soc.* **1975**, *97*, 7490. (f) Davidson, J. L.; Green, M.; Stone, F. G. A.; Welch, A. J. *J. Chem. Soc., Dalton Trans.* **1979**, 506. (g) Brice, M. D.; Dellaca, R. J.; Penfold, B. R.; Spencer, J. L. *J. Chem. Soc., Chem. Commun.* **1971**, 72. (h) Robinson, B. H.; Spencer, J. L. *J. Organomet. Chem.* **1971**, *33*, 97.

(6) (a) Gallop, M. A.; Housecroft, C. E.; Johnson, B. F. G.; Lewis, J.; Owen, S. M.; Raithby, P. R.; Wright, A. H., preceding paper in this issue. (b) Gomez-Sal, M. P.; Johnson, B. F. G.; Lewis, J.; Raithby, P. R.; Wright, A. H. *J. Chem. Soc., Chem. Commun.* **1985**, 1682. (c) Gallop, M. A.; Johnson, B. F. G.; Lewis, J.; Raithby, P. R. *J. Chem. Soc., Chem. Commun.* **1987**, 1809. (d) Gallop, M. A.; Johnson, B. F. G.; Lewis, J.; McCamley, A.; Perutz, R. N. *J. Chem. Soc., Chem. Commun.* **1988**, 1071.

0002-7863/92/1514-2510$03.00/0

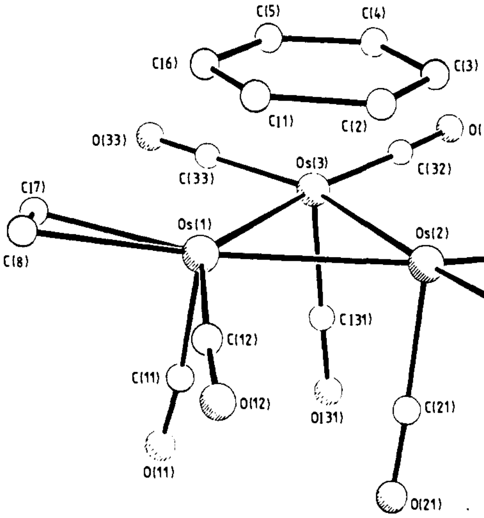

Figure 1. The molecular structure of $[Os_3(CO)_8(\eta^2\text{-}CH_2CH_2)(\mu_3:\eta^2:\eta^2:\eta^2\text{-}C_6H_6)]$ (**1**). Bond lengths: Os(2)–Os(1), 2.843 (1); Os(3)–Os(1), 2.858 (1); Os(3)–Os(2), 2.839 (1); Os(1)–C(1), 2.30 (2); Os(1)–C(6), 2.30 (2); Os(1)–C(7), 2.29 (3); Os(1)–C(8), 2.27 (3); Os(2)–C(2), 2.34 (2); Os(2)–C(3), 2.32 (2); Os(3)–C(4), 2.32 (3); Os(3)–C(5), 2.31 (2); C(2)–C(1), 1.50 (3); C(6)–C(1), 1.41 (3); C(3)–C(2), 1.44 (3); C(4)–C(3), 1.46 (3); C(5)–C(4), 1.38 (3); C(6)–C(5), 1.44 (4); C(7)–C(8), 1.39 (4).

illustrated in Figures 2 and 3, respectively (spectra for **3** and **4** are presented as supplementary material).

At ambient temperature the six inequivalent ring-protons in **1–4** (see time-averaged environments) showed broadened singlet resonances at ca. 4.0 ppm. Irradiating at the resonance frequency for free benzene (δ 7.35) in these spectra does not lead to saturation transfer to the coordinated ligand, demonstrating that the equilibrations are strictly intramolecular processes. The four ethylene protons in **1** show a single resonance at δ 2.03, while three olefinic proton multiplets may be clearly identified in the spectra of **3** and **4**. Their assignments are made straightforwardly on the basis of observed J couplings. The olefinic resonances in the propene complex **2** at 293 K are virtually isochronous and consequently show strongly second-order multiplet effects. No saturation transfer is observed to the coordinated ethylene on irradiation at the free ligand frequency, again repudiating the existence of a rapid dissociative equilibrium with a coordinatively unsaturated species.

Under conditions of slow exchange the benzene ligand in **1–4** gives rise to six pseudo-triplet resonances, with an accidental degeneracy evident in the spectra of **1**, **2**, and **4**. A most remarkable feature of these spectra is the substantial shielding (2–3 ppm) of a single ring proton in each complex (cf. the static spectra of $[(\mu\text{-}H)Os_3(CO)_8(PPh_3)(\mu_3:\eta^2:\eta^2:\eta^2\text{-}C_6H_6)][BF_4]$[6a] and $[H(\mu\text{-}H)Os_3(CO)_8(\mu_3:\eta^2:\eta^2:\eta^2\text{-}C_6H_6)]$[7] where the ^1H resonances of the face-capping benzene span, respectively, 1.3 and 0.6 ppm). Clearly this effect may be directly attributed to the presence of the π-bound olefin moiety in **1–4** and in each case the high field resonances are assigned to the ring protons H_6 lying proximal to the alkene ligand. That the olefin complexes exhibit higher ring-proton coalescence temperatures than the neutral phosphine derivatives[6a] $[Os_3(CO)_8(PR_3)(\mu_3:\eta^2:\eta^2:\eta^2\text{-}C_6H_6)]$, R = Et, Ph, o-tolyl, probably reflects a combination of this broader frequency dispersion in the static spectra of the former compounds, together with higher activation barriers to ring rotation due to the greater *effective* steric bulk of the alkene moieties.

One proton of the olefin ligand also suffers a substantial upfield shift in the static spectra of each of **1–4**. This shift is most obvious in ethylene complex **1** (viz. the pseudotriplet at δ 0.72 in Figure 2) but becomes apparent in **2–4** when it is noted that, almost invariably,[8] proton H_A geminal to the substituent group in low-valent transition-metal π-complexes of propene,[9] styrene,[9,10] and neohexene[9b,11] is deshielded with respect to the β-proton pair H_B and H_C.

This trend is reversed in the triosmium clusters **2–4**, where H_A persistently resonates at highest field in the *slow-exchange* spectra.

We believe that these shieldings have a common origin and account for the effect in terms of magnetic anisotropy associated with two (formally) metallacyclopropane rings. The shielding effects of cyclopropane and heterocyclopropane rings on neighboring protons in organic molecules are well established, and calculations based on a ring current model invoking cyclic σ-electron delocalization in the three-membered systems have accurately reproduced the observed shieldings.[12] Protons H_6 and H_A lie directly above metallacycles formed by the metal–olefin and metal–arene interactions respectively.

From shielding maps produced by the ring current model this is precisely the region for which large upfield shifts are anticipated. The coordination shifts of olefins and arenes have been frequently discussed in terms of anisotropy of the metal–ligand bonding,[13] and the attendant spatial variation of shielding in the vicinity of such π-bonded systems noted by other workers.[14]

Dynamic Isomerization of Substituted Olefin Complexes. Ten distinct resonances are found in the low temperature limiting ^1H spectrum of the ethylene derivative **1**, consistent with the solid-state structure established crystallographically (Figure 1). Four diastereomeric forms of the substituted complexes **2–4** are anticipated since the prochiral olefins may coordinate to the cluster via inequivalent *re* or *si* faces, and in each mode there exists two rotameric "in-plane" conformations for the bound ligand. Significantly, the olefinic region of the low temperature spectra of **2–4** is dominated by a single set of ligand resonances, indicating that one conformation of the coordinated alkene is distinctly favored in the static limit. The shielding arguments presented above are taken as evidence that these low-energy conformers are essentially isostructural and adopt the orientation shown above.

This assignment is corroborated for styrene complex **3** by two-dimensional CAMELSPIN spectroscopy (supplementary material).[15] At the temperatures needed to achieve slow-exchange limiting spectra for **1–4** the solutions are highly viscous, and this leads to long molecular correlation times for the complexes (i.e., $\omega_0\tau_c > 1$, ω_0 = Larmor frequency).[16] In this limit, strong negative NOE enhancements are expected which are indistinguishable from chemical exchange effects in NOESY or steady-state NOE experiments. In contrast, NOE cross-peaks are always positive in CAMELSPIN spectra, whereas chemical exchange peaks are negative.[15] A CAMELSPIN spectrum can therefore distinguish

---

(7) Gallop, M. A.; Johnson, B. F. G.; Lewis, J., unpublished observations.

(8) Werner, H.; Feser, R. *J. Organomet. Chem.* **1982**, *232*, 351.

(9) (a) Kiel, W. A.; Lin, G.-Y.; Bodner, G. S.; Gladyz, J. A. *J. Am. Chem. Soc.* **1983**, *105*, 4958. (b) Lemkuhl, H.; Naydowski, C.; Danowski, F.; Bellenbaum, M.; Benn, R.; Rufinska, A.; Schroth, G.; Mynott, R.; von Stanislow Pasynkiewicz, M. *Chem. Ber.* **1984**, *117*, 3231.

(10) (a) Lemkuhl, H.; Grundke, J.; Schroth, G.; Benn, R. *Z. Naturforsch.* **1984**, *39B*, 1050. (b) Kremer, K. A. M.; Kuo, G.-H.; O'Connor, E. J.; Helquist, P.; Kerber, R. C. *J. Am. Chem. Soc.* **1982**, *104*, 6119. (c) Schmidt, E. K. G.; Dogan, M. *J. Organomet. Chem.* **1982**, *234*, 73.

(11) Guillot-Edelheit, G.; Chottard, J.-C. *J. Chem. Soc., Dalton Trans.* **1984**, 169.

(12) (a) Jackman, L. M.; Sternhill, S. *Applications of Nuclear Magnetic Resonance Spectroscopy in Organic Chemistry*; 2nd ed.; Pergamon: Oxford, 1969; pp 98–101, and references therein. (b) Poulter, C. D.; Boikess, R. S.; Brauman, J. I.; Winstein, S. *J. Am. Chem. Soc.* **1972**, *94*, 2291 and references therein.

(13) (a) Werner, H.; Werner, R. *J. Organomet. Chem.* **1980**, *194*, C7. (b) Bodner, G. M.; Todd, L. J. *Inorg. Chem.* **1974**, *13*, 360. (c) Graves, V.; Lagowski, J. J. *Inorg. Chem.* **1976**, *15*, 577. (d) Thoennes, D. J.; Williams, C. L.; Trahanovsky, W. S. *J. Magn. Reson.* **1974**, *13*, 18 and references therein. (e) Graves, V.; Lagowski, J. J. *J. Organomet. Chem.* **1976**, *120*, 397. (f) Farnell, L. F.; Randall, E. W.; Rosenberg, E. *J. Chem. Soc., Chem. Commun.* **1971**, 1078. (g) Mann, B. E.; Taylor, B. F. *^{13}C NMR Data for Organometallic Compounds*; Academic Press: London, 1981.

(14) (a) Elschenbroich, C.; Schneider, J.; Prinzbach, H.; Fessner, W.-D. *Organometallics* **1986**, *5*, 2091 and references therein. (b) Langer, E.; Lehner, H. *J. Organomet. Chem.* **1979**, *173*, 47.

(15) (a) Bothner-By, A. A.; Stephens, R. L.; Lee, J.; Warren, C. D.; Jeanloz, R. W. *J. Am. Chem. Soc.* **1984**, *106*, 811. (b) Bax, A.; Davies, D. G. *J. Magn. Reson.* **1985**, *63*, 207.

(16) Harris, R. K. *Nuclear Magnetic Resonance Spectroscopy*; Pitman: London, 1983.

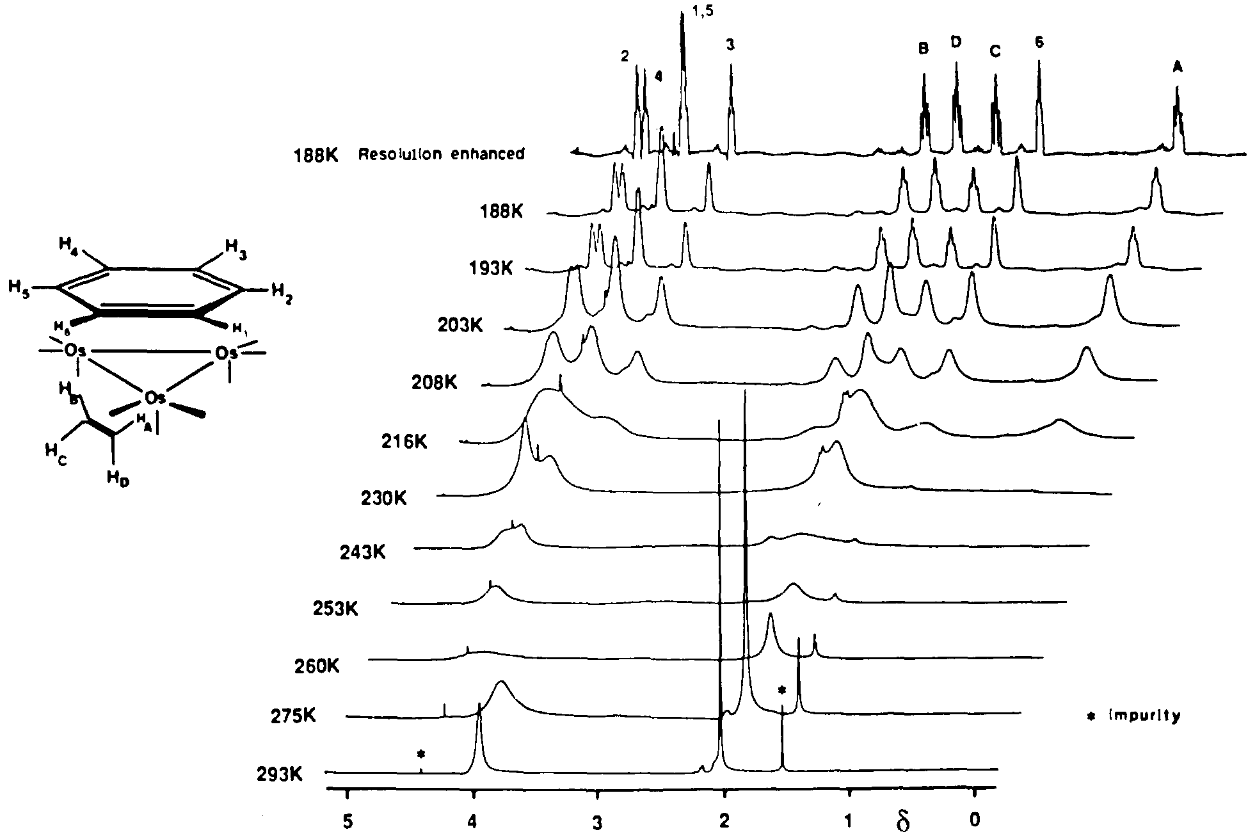

Figure 2. Variable temperature ^{1}H NMR spectra of $[Os_3(CO)_8(\eta^2\text{-}CH_2CH_2)(\mu_3\text{:}\eta^2\text{:}\eta^2\text{:}\eta^2\text{-}C_6H_6)]$ (1).

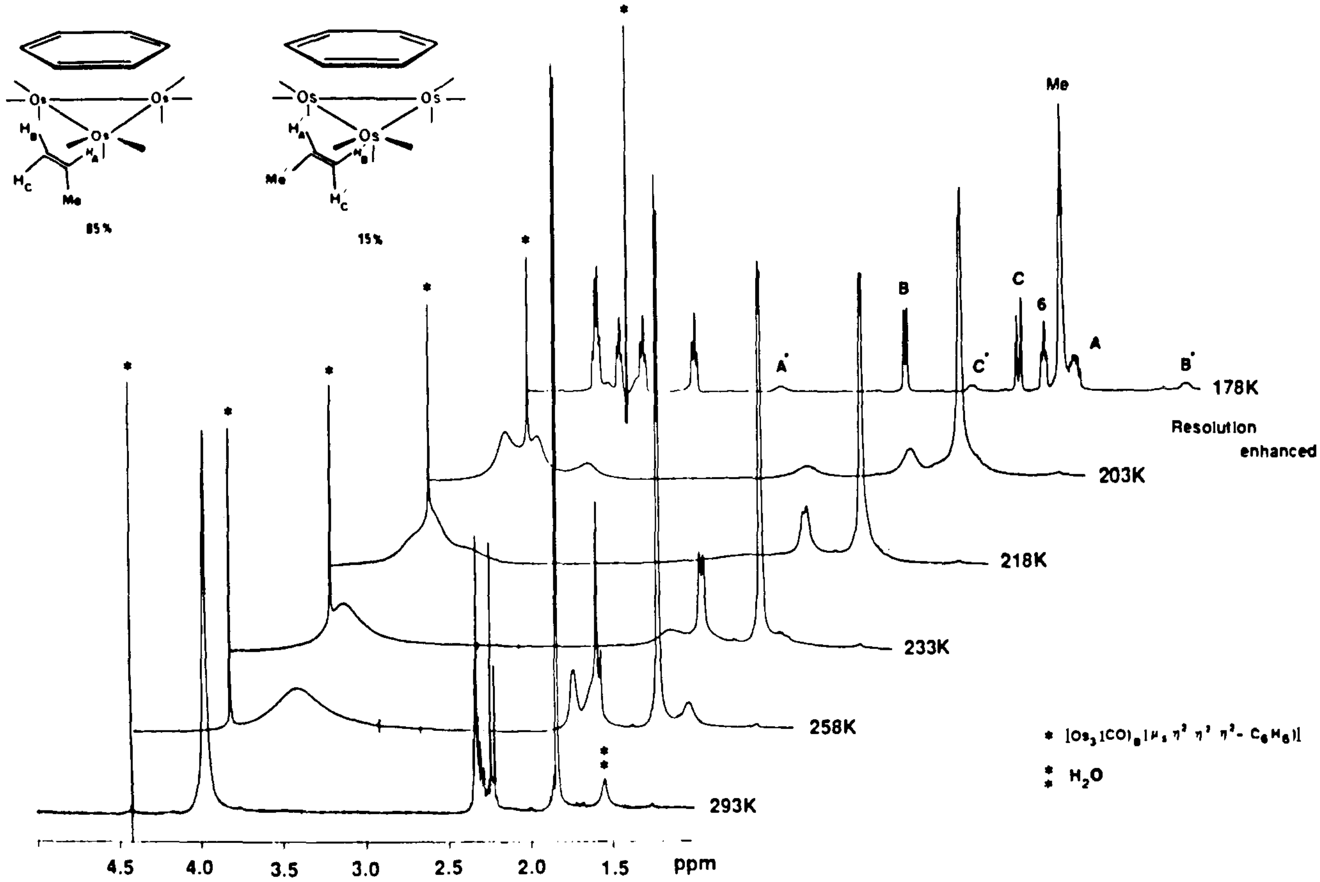

Figure 3. Variable temperature ^{1}H NMR spectra of $[Os_3(CO)_8(\eta^2\text{-}CH_2CHMe)(\mu_3\text{:}\eta^2\text{:}\eta^2\text{:}\eta^2\text{-}C_6H_6)]$ (2).

the two effects, and NOE enhancements are seen between the olefin protons H_A and H_B to the proximal benzene proton H_6, indicating that the substituent phenyl group is directed away from the face-capping ligand.

For the propene complex **2** three olefinic resonances of a minor diastereomer **2a**, present to the extent of ca. 15%, are clearly visible in the low temperature spectrum (Figure 3), and the upfield shift seen for H_B in this isomer suggests the structural assignment below.

Note that H_A resonates downfield (δ 3.45) in **2a** as expected, emphasizing again the marked anisotropy of the metal–benzene interaction. **2** and **2a** are nonrotameric diastereomers, and their rapid interconversion at 293 K implicates some polytopal rearrangement of the $Os(CO)_2$(olefin) fragment. Together with Cramer-type olefin rotation about the $Os–CH_2CH_2$ axis,[2c,17] this process must contribute to the equilibration of all four ethylene protons in **1** since either process alone could only lead to pairwise exchange of the C_2H_4 protons (vide infra).

There is no evidence for the presence of rotamers of the lower energy isomers **2** and **2a** in the ^1H NMR spectrum of the propene complex at 178 K (we estimate a lower limit to detection of ca. 2–3%).[18] Steric interactions between the olefin substituent and benzene ring protons could account for the destabilization of these alternative conformers and clearly such discrimination should be sensitive to the bulk of the substituent group.

Two very low intensity multiplets (~3%) observed in the static spectrum of **3** at δ 3.20 and δ 3.11 are attributed to styrene proton H_C in two minor conformers, since on irradiation of each the H_C resonance in the major isomer is denuded through saturation transfer. Other olefinic resonances in these higher energy diastereomers cannot be identified with confidence. By 293 K their contribution to the time-averaged styrene resonances must be substantial, however, as sizeable chemical shift differences from the slow-exchange spectrum are observed. In contrast, the olefin conformation in complex **4** is effectively locked by virtue of the steric bulk of the *^{t}Bu* group; i.e., any alternative diastereomer is sufficiently destabilized that its equilibrium concentration is low over the entire temperature range investigated, with only minor exchange broadening effects being observed.

Ring-Proton Assignment. Detailed assignments of the static ^1H NMR spectra of styrene complex **3** (the only derivative in which all the ring-proton resonances are resolved) and the parent compound **1** have been realized through a combination of two-dimensional homonuclear correlation spectroscopy (COSY) and spin–lattice relaxation time measurements. The double-quantum-filtered COSY spectrum of **3**, recorded at 183 K, is illustrated in Figure 4. Off-diagonal cross-peaks correlate nuclei that share a scalar coupling, and among the ring protons it is only the vicinal coupling constants ($^3J_{HH}$) that are sufficiently large to be detected in this experiment. Thus the high field resonance (H_6) is correlated with adjacent protons H_1/H_5, and the coupling network may be traced through the remaining protons H_2–H_4.

Protons H_1 and H_5 may be distinguished on the basis of their spin–lattice relaxation times (see Table I), measured at 198 K using the inversion-recovery technique. A comparison of the ring-proton T_1 values indicate anomalously rapid relaxation for H_6 (T_1 = 0.51 ± 0.01 s) and for the proton resonating at δ 4.52 (i.e., either H_1 or H_5; T_1 = 0.74 ± 0.01 s). Intramolecular dipole–dipole interaction provides the dominant mechanism for proton relaxation and its efficiency depends markedly on the internuclear separation between cross-relaxing nuclei.[16] Clearly H_1 and H_6 most closely approach protons of the olefin ligand (H_A and H_B) in these complexes (cf. X-ray structure of **1**, and this spatial proximity provides the basis for the observed relaxation rate enhancements and for the assignment of H_1 (and hence the remaining ring nuclei).

The complete ^1H spectral assignment for styrene complex **3** is given in Table I. Note that the $^3J_{HH}$ are equal within experimental error, indicating that the μ_3-cyclohexatriene description of the face-capping ligand overestimates the extent of double bond localization in the ring here. Analogous experiments for the ethylene complex **1** permit only partial assignment of the limiting spectrum as the virtual isochrony of the resonances for H_1 and H_5 precludes their distinction. Olefin mobility in **1** leads to time-averaged symmetrization of the complex (vide infra), however, and the remaining resonances may still be assigned without ambiguity (Table I).

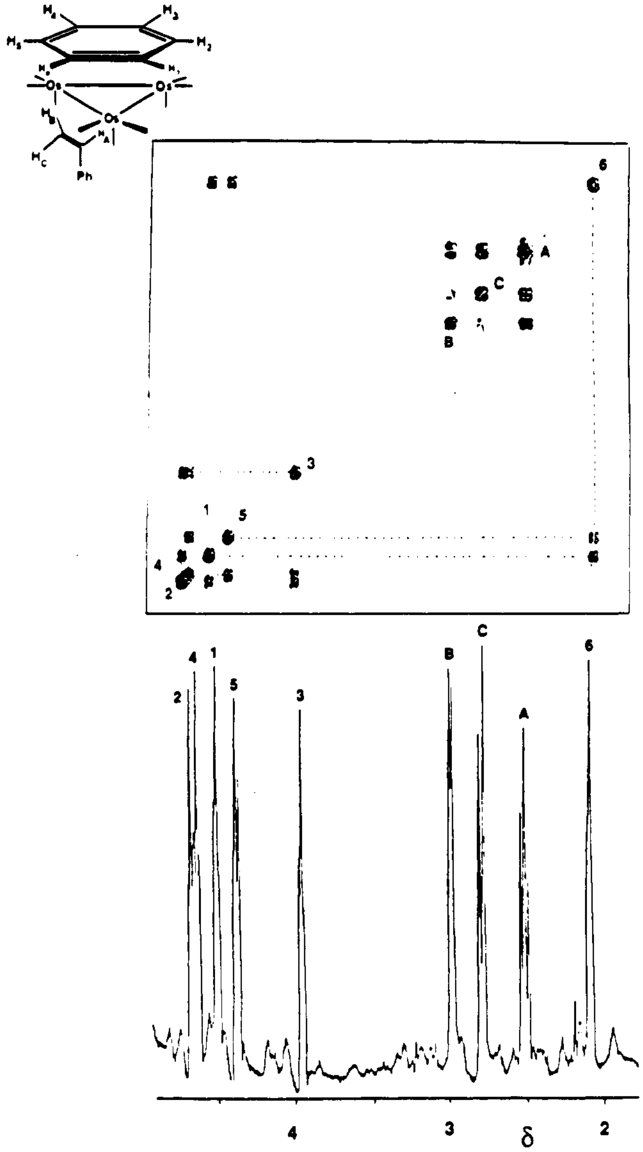

Figure 4. ^1H DQF-COSY spectrum of $[Os_3(CO)_8(\eta^2\text{-}CH_2CHPh)(\mu_3\text{:}\eta^2\text{:}\eta^2\text{:}\eta^2\text{-}C_6H_6)]$ (**3**) with reference one-dimensional spectrum at 183 K.

^{13}C NMR Spectra of $[Os_3(CO)_8(\eta^2\text{-}CH_2CHR)(\mu_3\text{:}\eta^2\text{:}\eta^2\text{:}\eta^2\text{-}C_6H_6)]$. Variable temperature $^{13}C\{^1H\}$ NMR spectra for the ethylene and styrene complexes are shown in Figures 5–7. Low field spectra were recorded on material prepared from ^{13}CO-enriched $[Os_3(CO)_{12}]$ (30% statistical enrichment), while the upfield spectra in Figure 7 were acquired using styrene compound derived from ^{13}C-enriched benzene (ca. 2% per ring carbon). The ring-carbon and olefinic resonances in the low temperature limiting spectra (Figures 6 and 7) have been assigned via the heteronuclear ^1H–^{13}C chemical shift correlation experiment and the two-dimensional contour plot for complex **3** is illustrated in Figure 8.

Consider firstly the nonrigidity of the carbonyl ligand set in **1** (Figure 5). Two lines in the 292 K spectrum having integrated intensities 2:6 are attributed to CO ligands on the "front" (X) and "back" (Y, Z) osmium atoms, respectively. Values for $^1J(^{187}O–^{13}C)$ of ca. 118 Hz, measured from low-intensity satellites in the room temperature spectrum, rule out internuclear migration pathways for CO equilibration, but implicate localized ligand interchange processes at the individual metal centers.[19]

The activation barriers to these processes are well separated

---

(17) (a) Cramer, R. *J. Am. Chem. Soc.* **1964**, *86*, 217. (b) Cramer, R. *J. Am. Chem. Soc.* **1967**, *89*, 5377. (c) Cramer, R.; Kline, J. B.; Roberts, J. D. *J. Am. Chem. Soc.* **1969**, *91*, 2519.

(18) It must be remembered, however, that the resonances of a minor component may be substantially broader than those of the major species, as the rate of its isomerization is necessarily higher to preserve equilibrium.

(19) Gallop, M. A.; Johnson, B. F. G.; Lewis, J. *J. Chem. Soc., Chem. Commun.* **1987**, 1831.

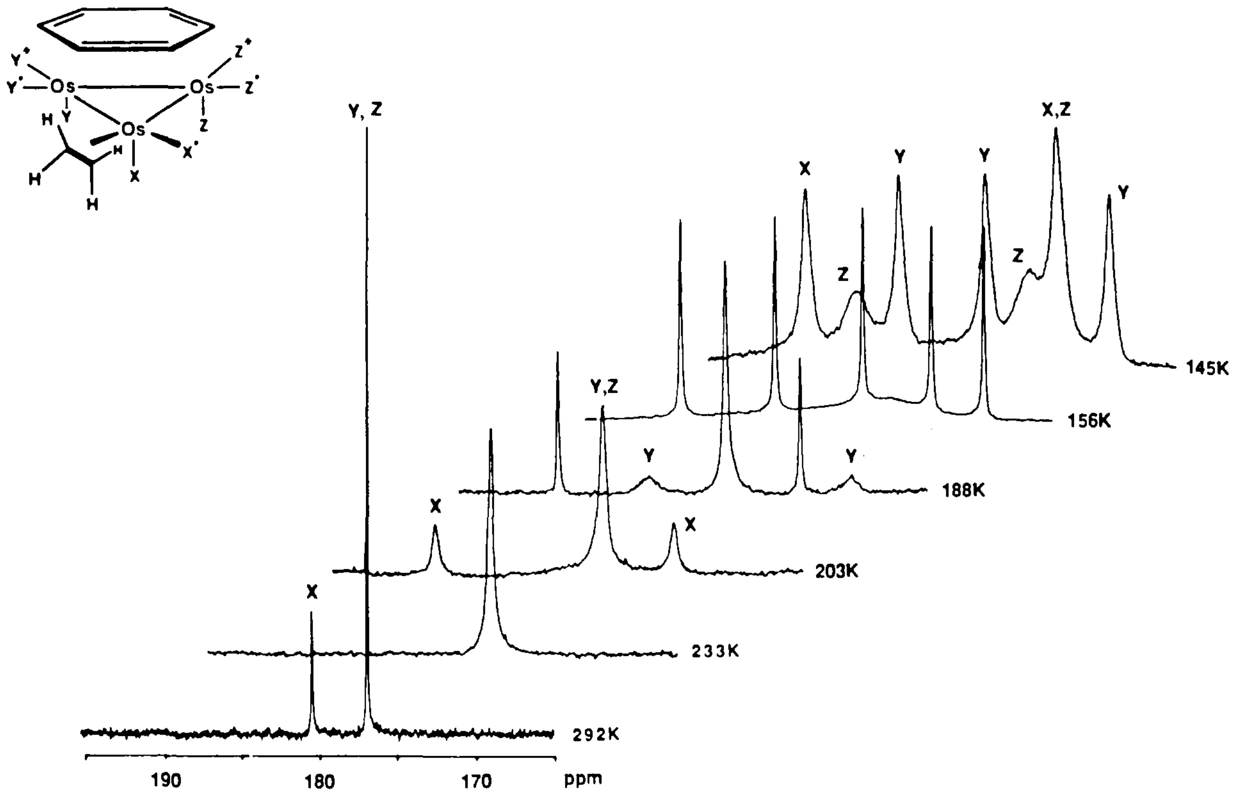

Figure 5. Variable temperature $^{13}C\{^1H\}$ NMR (downfield) spectra of $[Os_3(CO)_8(\eta^2\text{-}CH_2CH_2)(\mu_3\text{:}\eta^2\text{:}\eta^2\text{:}\eta^2\text{-}C_6H_6)]$ (1).

and three distinct coalescence phenomena are observed. Of highest energy is the rearrangement of the $Os(CO)_2(\eta^2\text{-}CH_2CH_2)$ polytope (T_C = 232 K); this pathway, termed olefin site-exchange, permutes the olefin and CO ligands X/X′ and, importantly, introduces a mirror plane of symmetry into 1.

It is this time-averaged symmetrization that accounts for the degeneracy of the Y and Z resonances at 292 K and also equilibrates pairwise the olefin and benzene nuclei A/B, C/D and 1/6, 2/5, 3/4. Facile trigonal twists interchange carbonyls within the Y and Z sets, and we suggest that steric hindrance to fluxionality provides resonable grounds for assigning COs in the higher energy rearrangement (T_C ~ 192 K) to the proximal Y ligands. Fluxionality within the Z set is not fully suppressed, even at 145 K (in $CD_2Cl_2/CHFCl_2$), and the broadened lines reflect the glass-like nature of the solution at this temperature.

The temperature dependence of the low field ^{13}C NMR spectrum for styrene complex 3 (see supplementary data) resembles closely the behavior of the parent ethylene derivative, at least in a qualitative sense. An important distinction here is that, rather than symmetrizing the complex, styrene site-exchange effects an isomerization to a higher energy conformer, with the Y and Z carbonyl sets remaining distinct at all temperatures and the X/X′ resonances in the fast exchange limit appearing at the weighted-mean frequencies of the resonances of the component diastereomers in the equilibrium mixture. Recall that when R = ^tBu, any minor conformer is sufficiently destabilized that little exchange broadening of the olefinic resonances is observed in the variable temperature ^1H NMR spectra of 4. This effective conformational locking of the $Os(CO)_2$(olefin) polytope is also evident in the low field ^{13}C NMR spectrum of 4 where the X/X′ resonances suffer only slight exchange broadening over the temperature range 173–295 K.

Figures 6 and 7 illustrate the collapse of the ring-carbon resonances in 1 and 3, respectively, to broad, time-averaged lines on warming from the static limit to ambient temperature. Carbons 3 and 4 in the ethylene complex are accidentally isochronous and their combined resonance remains rather sharp until ca. 240 K, when exchange with the other benzene nuclei becomes apparent. The significance of this result is that the motions of the ring and olefin are *not* concerted, but that the barrier to fluxional rotation of the C_6 moiety is considerably greater than to "site-exchange" of the ethylene ligand in 1 (remember that C_3 and C_4 are related by the time-dependent plane of symmetry produced by ethylene migration). Cluster symmetrization is not relevant to the stereodynamic behavior of styrene derivative 3 and all six ring-carbon resonances broaden initially at the same rate (Figure 7). Two-dimensional exchange spectroscopy may be used to define unambiguously the mechanism of this exchange process (vide infra).

Mechanistic Aspects of Olefin Ligand Rearrangement. The preceding discussion of olefin ligand mobility has been primarily phenomenological: polytopal rearrangement at the $Os(CO)_2$(olefin) center interchanges axial and equatorial carbonyl ligands and effectively transfers the alkene between equatorial sites. Moreover, in ethylene complex 1, olefin rotation about the Os–CH_2CH_2 axis permutes trans related proton pairs H_A/H_C and H_B/H_D leading to complete ligand equilibration at 292 K. Such rotation may also contribute to a limited extent to the dynamic isomerization of the substituted olefin derivatives, particularly 2 and 3.

Additional mechanistic insight in the case of 1 comes from an analysis of coalescence data for the olefinic and carbonyl carbons (X/X′); coalescence temperatures of 219 and 232 K, respectively, yield approximate Eyring activation energies ΔG^*_{219} (CC) = 40.4 kJ mol^{-1} and ΔG^*_{232} (CO) = 40.6 kJ mol^{-1} for the two two-site exchanges. These barriers are certainly equal, within limits of experimental uncertainty, indicating that olefin rotation is at most only competitive with the site-exchange process, since the former pathway contributes to the equilibration of C_{AD}/C_{BC} without exchanging carbonyls X/X′. Qualitative spin saturation transfer experiments suggest further that the barrier to ethylene rotation exceeds that to localized ligand interchange, giving a lower limit of ~41 kJ mol^{-1} for the rotational process.

Figure 9 details several plausible pathways for interconversion of the four (equivalent) conformations I–IV of ethylene complex 1. Note that pure turnstile rotation of the $Os(CO)_2(CH_2CH_2)$ moiety should be characterized by two distinct rates (i.e., for processes (i) and (iii)) and that if the energy barriers for these routes are sufficiently dissimilar oscillation (or libration) of the ligand set may occur in preference to complete 360° rotation. The NMR technique does not distinguish between these possibilities but only provides information concerning the lowest energy pathway for a given site interchange.

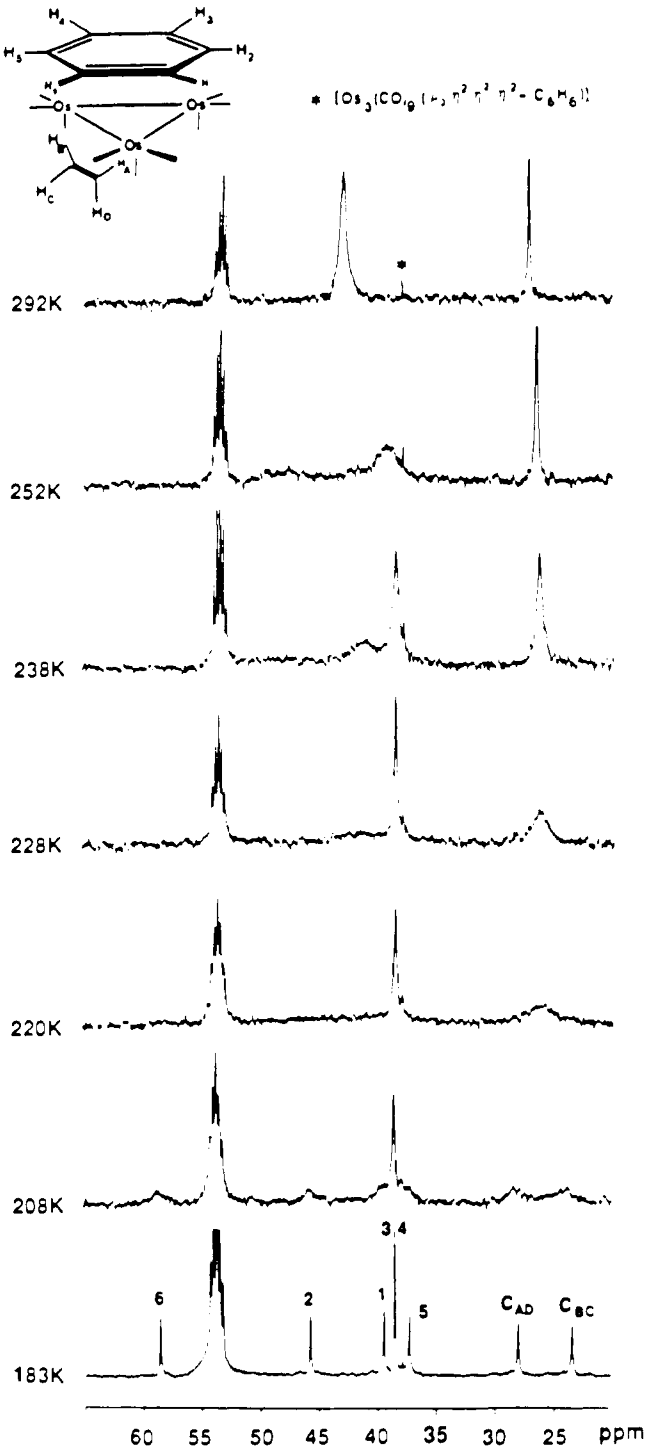

Figure 6. Variable temperature $^{13}C\{^1H\}$ NMR (upfield) spectra of $[Os_3(CO)_8(\eta^2\text{-}CH_2CH_2)(\mu_3\text{:}\eta^2\text{:}\eta^2\text{:}\eta^2\text{-}C_6H_6)]$ (**1**).

Pathway (iv) represents the concerted rotation and site-exchange of the ethylene ligand and taken together with (iii) could account for the stereodynamic behavior of **1**. Alternatively (iii) could be coupled with straightforward olefin rotation in the ground-state geometry (process (v) in Figure 9) as the higher energy pathway, leading to complete ligand equilibration. Site-exchange via (i) is a two-step process in which we envisage the intermediacy of axially substituted rotamers (V) and (VI). If these were sufficiently long-lived, then their interconversion through (ii) (with ΔG^* (ii) > ΔG^* (i)) could contribute to the fluxionality of **1**, though clearly process (v) could again effect olefin rotation here. Note that some olefin libration is required to maintain maximum metal–ligand π-overlap throughout site-exchange.

The precise rearrangement mechanism pursued will doubtlessly reflect the pathway in which destabilizing steric and electronic

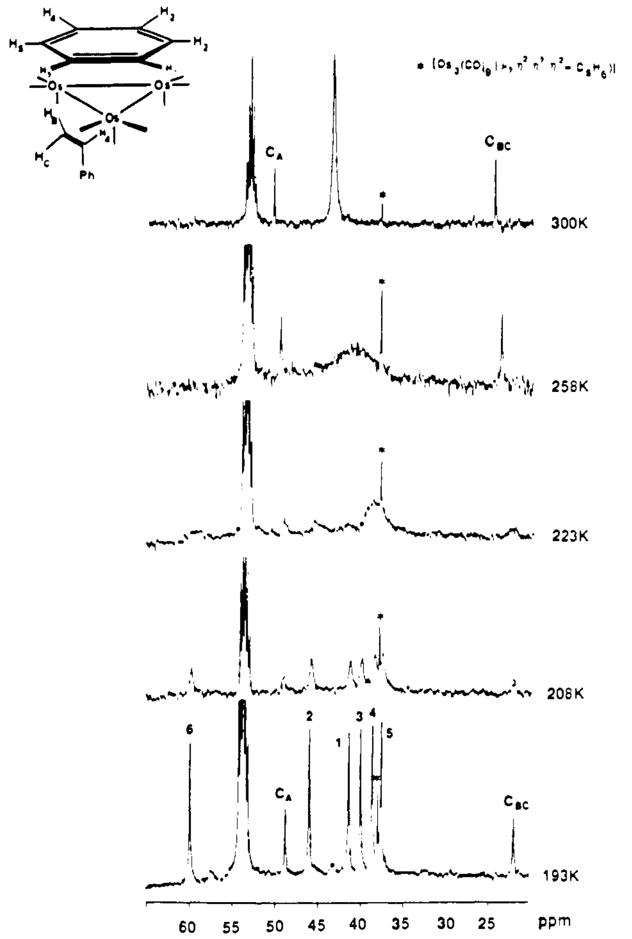

Figure 7. Variable temperature $^{13}C\{^1H\}$ NMR (upfield) spectra of $[Os_3(CO)_8(\eta^2\text{-}CH_2CHPh)(\mu_3\text{:}\eta^2\text{:}\eta^2\text{:}\eta^2\text{-}C_6H_6)]$ (**3**).

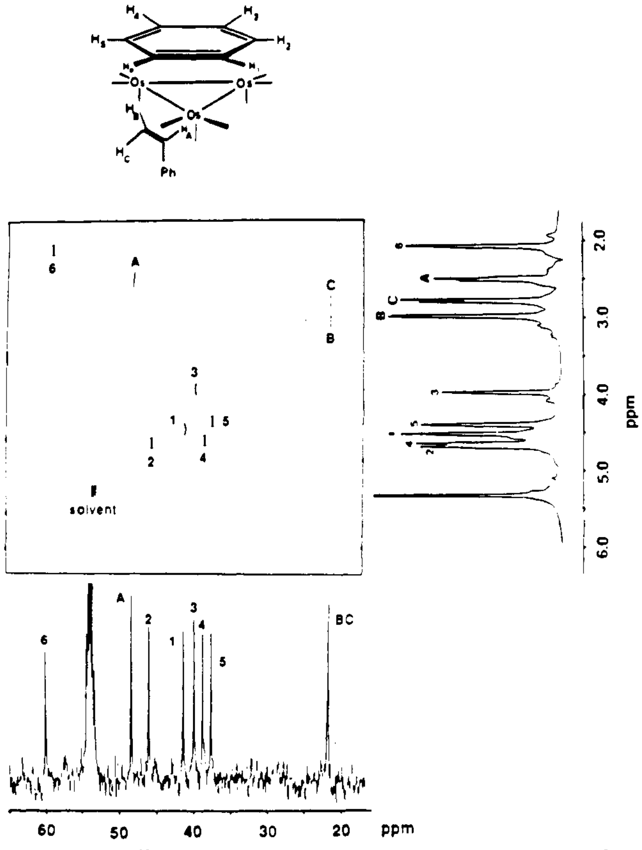

Figure 8. $^1H\text{-}^{13}C$ chemical shift correlation spectrum of $[Os_3(CO)_8(\eta^2\text{-}CH_2CHPh)(\mu_3\text{:}\eta^2\text{:}\eta^2\text{:}\eta^2\text{-}C_6H_6)]$ (**3**) with reference one-dimensional spectra at 183 K.

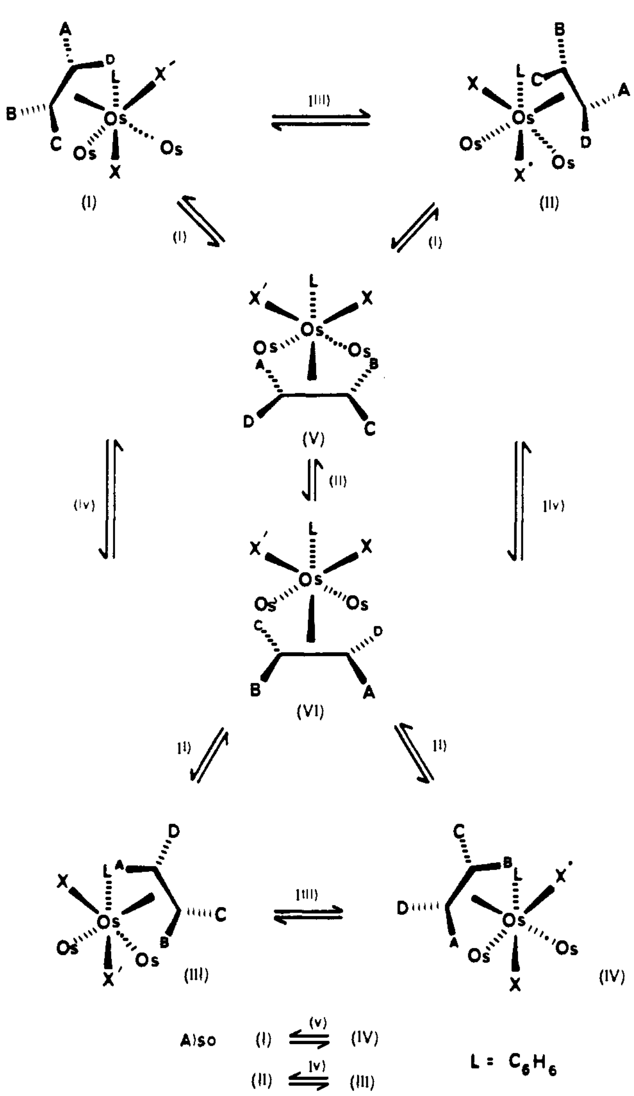

Figure 9. Possible olefin ligand migration pathways for $[Os_3(CO)_8(\eta^2\text{-}CH_2CH_2)(\mu_3{:}\eta^2{:}\eta^2{:}\eta^2\text{-}C_6H_6)]$ (**1**).

effects are minimized. Restricted trigonal twists, according to process (iii), have been recently proposed by Pomeroy[20] to rationalize the migration of a phosphite ligand between equatorial coordination sites in triosmium clusters, without requiring the bulky ligand to enter an axial site where steric hindrance from two axial carbonyls would be encountered. It seems reasonable that in **1** the eclipsing of benzene and olefin ligands in the transition state for process (iii) may prove sufficiently unfavorable that the two-step site-exchange pathway (i) is preferred. Indeed, a reduced barrier to ethylene rotation in the intermediate axial conformations V and VI is anticipated on electronic grounds, since the direct competition with the trans related arene ligand for overlap with metal-based orbitals should diminish π-back bonding to the olefin.[21] Intimate coupling of olefin rotation and carbonyl ligand scrambling (including the turnstile process) has been previously recognized in the fluxional behavior of mononuclear metal complexes.[22]

Two-Dimensional $^{13}C\{^1H\}$ Exchange Spectroscopy of $[Os_3(CO)_8(\eta^2\text{-}CH_2CHPh)(\mu_3{:}\eta^2{:}\eta^2{:}\eta^2\text{-}C_6H_6)]$. Magnetization transfer as occurs in the nuclear Overhauser effect or in chemical exchange processes may be followed efficiently using two-dimensional NMR spectroscopy. The approach, first proposed by Jeener[23] in 1979, has become well established in recent years as a powerful tool for the investigation of conformational behavior of biological macromolecules, where the method is known as NOESY (nuclear Overhauser effect spectroscopy).[24] When the NOESY procedure is applied to the study of chemical exchange it is more appropriately termed EXSY (exchange spectroscopy) and to date some 10–15 EXSY investigations of isomerization and fluxionality in organometallic complexes have appeared in the literature.[25] The real advantage of this two-dimensional methodology over conventional one-dimensional magnetization transfer techniques becomes apparent for multisite problems, since the need to selectively excite individual resonances in the spectrum is removed and all the exchange information is contained in a single experiment. In addition to establishing exchange pathways, it is desirable to extract numerical values of the rate constants for the underlying processes. The most satisfactory treatment devised is due to Abel, Orrell, and co-workers in which direct evaluation of the rate constants from a single EXSY spectrum is possible for a multisite system of any complexity.[26]

We have applied the ^{13}C two-dimensional EXSY technique to the analysis of the fluxional behavior of the μ_3-benzene ligand in $[Os_3(CO)_8(\eta^2\text{-}CH_2CHPh)(\mu_3{:}\eta^2{:}\eta^2{:}\eta^2\text{-}C_6H_6)]$ (**3**) near the slow exchange limit and have determined rate constants for the exchange process. The rather poor solubility of **3** at this low temperature necessitated partial ^{13}C enrichment of the μ_3-ligand; material for this experiment was derived from benzene selectively enriched to the extent of ca. 30% at one carbon atom per molecule giving a statistical 5-fold enrichment at each ring carbon in the cluster complex. Figure 10 illustrates the contour plot of the $^{13}C\{^1H\}$ EXSY spectrum for styrene complex **3**, acquired at 211 K with $\tau_{mix} = 0.11$ s. Magnetization transfer clearly occurs between each ring carbon nucleus and (predominantly) its two nearest neighbours through chemical exchange during τ_{mix}. A typical section through a diagonal peak, corresponding to the signal for C_2, is also shown in Figure 10 and reveals weak cross-peaks at the resonance frequencies for C_4 and C_6 in addition to the primary correlations with C_1 and C_3. Integrated intensities of all these diagonal and cross-peaks are given as supplementary material.

Analysis of these data using the program D2DNMR[26] yields just one distinct rate constant, k, for benzene migration, where $k = k_{12} = k_{23} = k_{34} = k_{45} = k_{56} = k_{61} = 5 \pm 1\ s^{-1}$, all other k_{ij} not being significantly different from zero. The principal source of error in k arises from unreliable peak integration reflecting poor signal-to-noise in the rows and columns of the two-dimensional spectrum. EXSY spectra for **3** have also been recorded at 211 K using mixing times of 0.06 and 0.20 s, and the data from these experiments agree closely with peak intensities calculated on the basis of a single rate constant, $k \sim 5\ s^{-1}$. Substitution for k into the Eyring expression provides an activation free-energy $\Delta G^*_{211} = 48.3 \pm 0.3$ kJ mol^{-1} for ring rotation.

We have demonstrated, then, that the primary mechanism for fluxional ring rotation in **3** at this temperature involves permutation of the C_6 moiety via a series of 1,2 shifts relative to the basal metal triangle, as illustrated in Figure 9.

It seems likely that this least-motion pathway of 1,2 ring shifts also accounts for the nonrigidity of other μ_3-benzene complexes in our studies, and it is noteworthy that the dynamic behavior of many polyene and polyenyl metal complexes may be interpreted

---

(20) (a) Alex, R. F.; Pomeroy, R. K. *J. Organomet. Chem.* **1985**, *284*, 379. (b) Alex, R. F.; Pomeroy, R. K. *Organometallics* **1987**, *6*, 2437.

(21) Kiel, G.-Y.; Takats, J.; Grevels, F.-W. *J. Am. Chem. Soc.* **1987**, *109*, 2227.

(22) (a) Faller, J. W. *Adv. Organomet. Chem.* **1977**, *16*, 211. (b) Howell, J. A. S. In *Advances in Dynamic Stereochemistry*; Gielen, M. F., Ed.; Freund: London, 1985; Vol. 1. (c) Kreiter, C. G.; Lang, M. J. *J. Organomet. Chem.* **1973**, *55*, C27. (d) Kreiter, C. G.; Stueber, S.; Wackerle, L. *J. Organomet. Chem.* **1974**, *66*, C49. (e) Albright, T. A.; Hoffmann, R.; Thibeault, J. C.; Thorn, D. L. *J. Am. Chem. Soc.* **1979**, *101*, 3801 and references therein.

(23) Jeener, J.; Meier, B. H.; Bachmann, P.; Ernst, R. R. *J. Chem. Phys.* **1979**, *71*, 4546.

(24) (a) Kumar, A.; Wagner, G.; Ernst, R. R.; Wuthrich, K. *J. Am. Chem. Soc.* **1981**, *103*, 3654. (b) Wilder, G.; Macura, S.; Kumar, A.; Ernst, R. R.; Wuthrich, K. *J. Magn. Reson.* **1984**, *56*, 207.

(25) (a) Aguero, A.; Butler, I. S.; Ismail, A. A.; Sauriol, F. In *Advances in Dynamic Stereochemistry*; Gielen, M. F., Ed.; Freund: Vol. 2, in press, and references therein. (b) Bandy, J. A.; Green, M. L. H.; O'Hare, D. *J. Chem. Soc., Dalton Trans.* **1986**, 2477.

(26) Abel, E. W.; Coston, T. P. J.; Orrell, K. G.; Sik, V.; Stephenson, D. *J. Magn. Reson.* **1986**, *70*, 34.

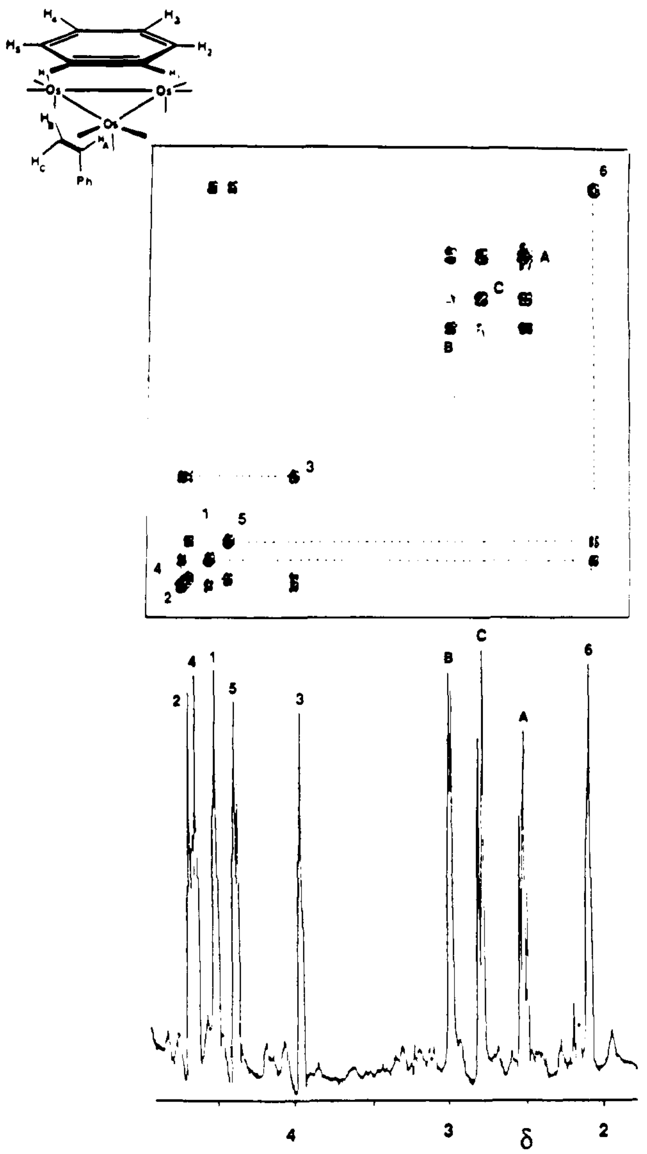

Figure 10. $^{13}C\{^1H\}$ two-dimensional EXSY spectrum of $[Os_3(CO)_8(\eta^2\text{-}CH_2CHPh)(\mu_3\text{:}\eta^2\text{:}\eta^2\text{:}\eta^2\text{-}C_6H_6)]$ (3) at 211 K, $\tau_{mix} = 0.11$ s. Reference one-dimensional spectrum shown at left, together with cross section through on-diagonal peak showing exchange correlations with carbon C_2.

in terms of a 1,2 shift mechanism for metal migration.[2a] Mingos[28] has developed a theoretical model for this behavior based on the Woodward–Hoffmann rules of organic chemistry; the least-motion shift in a $(\eta^2\text{-}C_6R_6)$ complex, for example, may be regarded as a 1,5 suprafacial sigmatropic shift of one of the metal–arene bonds in a valence bond representation of this system. This process is fully allowed by the criterion of conservation of orbital symmetry and is consequently facile (e.g., 1,2 metal shifts occur in $[Pt(\eta^2\text{-}C_6(CF_3)_6)(PEt_3)_2]$ with $\Delta G^* \sim 45$ kJ mol^{-1}).[29]

An important lesson from this analysis is that some caution must be exercised in qualitatively interpreting complex EXSY spectra in terms of various possible exchange pathways. While the 1,2 shift mechanism for 3 could have been anticipated from the two-dimensional spectrum by inspection, the existence of additional weak cross-peaks does *not* necessarily imply a second direct exchange pathway between the sites in question. Rather, these peaks arise from indirect exchange (i.e., successive 1,2 shifts) during τ_{mix} and, in principle, any qualitatively accessible information may be removed from an EXSY spectrum if excessive mixing times are used.

The importance of choosing optimal mixing times in quantitative two-dimensional EXSY experiments has also been stressed by several workers.[25a,26] A too short mixing time, compared with the lifetime of the nuclei in one site, would result in very small exchange cross-peaks, while excessively long τ_{mix} may lead to signal intensities becoming insensitive to exchange rates. Alternatively, if the spin–lattice relaxation rates are fast relative to exchange, then all signals lose intensity appreciably during long mixing times. This balance is particularly fine in the case of styrene complex 3, where the T_1's are short and unacceptable exchange-broadening occurs at temperatures much above 210 K.

The $^{13}C\{^1H\}$ EXSY spectrum of the parent ethylene complex 1 (198 K, $\tau_{mix} = 0.03$ s) shows correlation only between pairs of carbon nuclei related by the effective symmetry plane introduced by ethylene site-exchange. This result could have been anticipated from the variable temperature one-dimensional spectra (Figure 6) since at 198 K fluxional rotation of the μ_3-benzene contributes negligibly to exchange-broadening of the carbon resonances.

Fluxionality of $[Os_3(CO)_8(\eta^2\text{-}CH_2CH_2)(\mu_3\text{:}\eta^2\text{:}\eta^2\text{:}\eta^2\text{-}C_6H_6)]$ in the Solid State. It is of interest to know whether the fluxional processes identified by these solution NMR studies persist in the solid state, and if they do, to what extent the activation barriers differ from those that pertain in solution. In fact it is becoming increasingly apparent from variable temperature solid state NMR studies of metal clusters and other organometallic compounds that neither molecular reorientation nor ligand exchange processes are necessarily precluded by lattice interactions in the solid state.[30] For example, the fluxionality of solid binary metal carbonyl complexes has been discussed in terms of polytopal reorganizations of ligand polyhedra[1a,31] or of metal core rotations within CO polytopes.[32] In pioneering studies Fyfe and co-workers detected ring hopping in $(\eta^1\text{-}C_5H_5)$M moieties by wideline ^{1}H NMR[33] and ring rotations of coordinated cyclooctatetraene in the complexes $[Fe(CO)_3(\eta^4\text{-}C_8H_8)]$, $[Fe_2(CO)_5(\mu\text{:}\eta^8\text{-}C_8H_8)]$, and $[Ru_3(CO)_4(\mu\text{:}\eta^8\text{-}C_8H_8)_2]$ both by ^{1}H wideline and ^{13}C CP/MAS NMR.[4c,34] Delise et al.[35] have claimed an activation barrier for benzene reorientation about its principal axis in solid $[Cr(CO)_3(\eta^6\text{-}C_6H_6)]$ of ca. 14 kJ mol^{-1}, while ^{13}C CP/MAS spectra of $[M(CO)_3(\eta^6\text{-}C_6H_5Me)]$, M = Cr, Mo, are consistent with rigidity of the substituted arene but rotational motion of the tricarbonyl group.[36] Diene topomerization in $[Zr(\eta^5\text{-}C_5H_4Bu^t)_2(CH_2{=}CHCH{=}CH_2)]$ has recently been established by ^{13}C CP/MAS two-dimensional exchange spectroscopy.[37] By comparison, X-ray diffraction techniques are frequently insensitive to solid state dynamic behavior unless orientational disorder is introduced or low frequency motion is detected in the form of large atomic thermal parameters.[38] Correlations between low activation energy dynamic processes in clusters observed by MAS and solution NMR with mean square displacement (msd) parameters obtained from crystallographic studies have recently been made.[39]

---

[27] Marion, D.; Wuthrich, K. *Biochem. Biophys. Res. Commun.* **1983**, *113*, 967.

[28] Mingos, D. M. P. *J. Chem. Soc., Dalton Trans.* **1977**, 31.

[29] Browning, J.; Green, M.; Penfold, B. R.; Spencer, J. L.; Stone, F. G. A. *J. Chem. Soc., Chem. Commun.* **1973**, 31.

[30] (a) Hanson, B. E. In *Advances in Dynamic Stereochemistry*; Gielen, M. F., Ed.; Freund: London, 1985; Vol. 1. (b) Lyerla, J. R.; Yannoni, C. S.; Fyfe, C. A. *Acc. Chem. Res.* **1982**, *15*, 208.

[31] (a) Berry, R. S. *J. Chem. Phys.* **1960**, *32*, 933. (b) Johnson, B. F. G.; Benfield, R. E. *J. Chem. Soc., Dalton Trans.* **1978**, 1554. (c) Hansen, B. E.; Sullivan, M. J.; Davis, R. J. *J. Am. Chem. Soc.* **1984**, *106*, 251.

[32] (a) Dorn, H. C.; Hanson, B. E.; Motell, E. *Inorg. Chim. Acta* **1981**, *54*, L71. (b) Hanson, B. E.; Lisic, E. C.; Petty, J. T.; Iannacone, G. *Inorg. Chem.* **1986**, *25*, 4062. (c) Hanson, B. E.; Lisic, E. C. *Inorg. Chem.* **1986**, *25*, 716.

[33] (a) Campbell, A. J.; Fyfe, C. A.; Goel, R. G.; Maslowsky, E., Jr.; Senoff, C. V. *J. Am. Chem. Soc.* **1972**, *94*, 8387. (b) Campbell, A. J.; Cottrell, C. E.; Fyfe, C. A.; Jeffrey, K. R. *Inorg. Chem.* **1976**, *15*, 1326.

[34] (a) Campbell, A. J.; Fyfe, C. A.; Maslowsky, E., Jr. *J. Am. Chem. Soc.* **1972**, *94*, 2690. (b) Cottrell, C. E.; Fyfe, C. A.; Senoff, C. V. *J. Organomet. Chem.* **1972**, *43*, 203. (c) Campbell, A. J.; Cottrell, C. E.; Fyfe, C. A.; Jeffrey, K. R. *Inorg. Chem.* **1976**, *15*, 1321.

[35] Delise, P.; Allegra, G.; Mognaschi, E. R.; Chierico, A. *J. Chem. Soc., Faraday Trans. II* **1975**, *71*, 207.

[36] Wagner, G. E.; Hanson, B. E. *Inorg. Chem.* **1987**, *26*, 2019.

[37] Benn, R.; Grondey, H.; Nolte, R.; Erker, G. *Organometallics* **1988**, *7*, 777.

[38] Willis, B. T. M.; Pryor, A. W. *Thermal Vibrations in Crystallography*; Cambridge University Press: London, 1975.

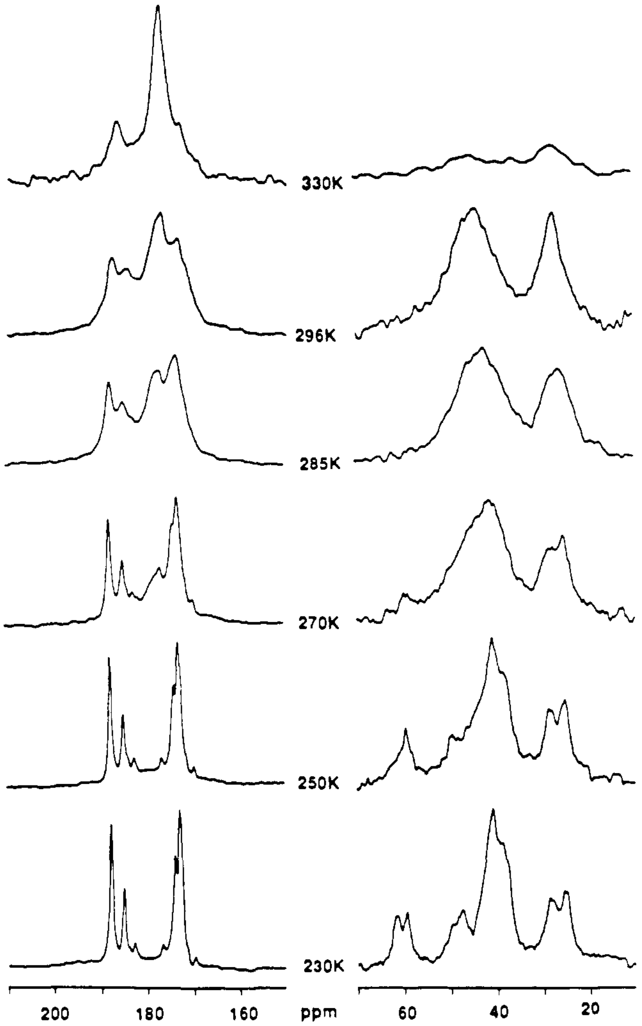

Figure 11. Variable temperature $^{13}C\{^1H\}$ CP/MAS spectra of $[Os_3(CO)_8(\eta^2\text{-}CH_2CH_2)(\mu_3\text{:}\eta^2\text{:}\eta^2\text{:}\eta^2\text{-}C_6H_6)]$ (**1**).

In Figure 11 preliminary $^{13}C\{^1H\}$ CP/MAS spectra of polycrystalline $[Os_3(CO)_8(\eta^2\text{-}CH_2CH_2)(\mu_3\text{:}\eta^2\text{:}\eta^2\text{:}\eta^2\text{-}C_6H_6)]$ (**1**) over the temperature range 230 to 330 K clearly indicate the occurrence of chemical exchange process(es) in the solid state. Resonances due to the benzene, ethylene, and carbonyl ligands are clearly distinguishable from each other, and within each subset it is possible to identify at least some individual carbon resonances (the observed line shape changes are completely reversible).[40] Importantly, extensive use is made of the ^{13}C solution NMR assignments in the analysis of the solid state NMR spectra, with the isotropic chemical shifts in the solid being closely similar (within ±3 ppm) to those in equivalent solution spectra.

We consider firstly the organic ligand region in Figure 11. Between 250 and 296 K the spectra broadly mirror the changes seen in the solution NMR (Figure 6), though the resolution is clearly much lower in the solid state. The spectrum at 250 K approaches the "slow" limit of the exchange-broadening regime, while at 296 K broad lines at ~44.5 and 27.6 ppm are attributed, respectively, to the resonances of six benzene and two ethylene carbons partially time-averaged by fluxional motion. However the new averaged resonances do not sharpen after coalescence as anticipated in the "fast" exchange limit but appear to be subjected to further broadening of a more extreme nature, increasing in severity from 270 K to a maximum at about 330 K where the resonances from the organic ligands are barely detectable. This difference between the solid state and solution spectra occurs because in solids the motional processes may interfere with interactions arising from aspects of the CP/MAS experiment other than just the exchange broadening due to chemical shift averaging. Specifically, since the sample is under the influence of a high power ^1H dipolar decoupling field (ω_1 = 71 kHz), a region of broadening is expected when the molecular motional frequencies match this rf decoupling field strength.[41] Note that the carbonyl spins experience a smaller line-broadening effect since they are more weakly dipolar coupled to the proton reservoir ($1/T_2 \propto 1/r^6$). Motional interference on the time scale of the magic angle sample spinning[43] is unlikely to provide the dominant mechanism for this line-broadening due to the rather small chemical shift anisotropy (CSA) of the organic ligands and to the relatively high MAS speed employed (~4.5 kHz). Estimating the temperature of maximum broadening for both the benzene and ethylene resonances to be ~330 K yields an approximate Eyring activation energy for the motions of ΔG^*_{330} = 50.5 kJ mol^{-1}.

On cooling from 250 to 230 K the line shape changes in the upfield region of the solid state spectrum diverge from behavior in the solution spectrum, i.e., multiple resonances become resolved where only single lines are observed in solution. Particularly clear are the cases for the C_6 and C_2 resonances of the benzene ligand (i.e., at 60 and 48 ppm) which show at least two distinct peaks spread over ~2–3 ppm and also each of the ethylene carbon resonances for which "doublet" splittings of ~40 Hz are seen. Since complex **1** crystallizes with one molecule in the asymmetric unit and has no crystallographically imposed symmetry,[6a] a one-to-one correspondence between magnetically distinguishable nuclei in the solution and solid phases would be anticipated.[44] One speculative explanation of these observations is that there may exist two or more NMR distinguishable conformations of the molecule or part of the molecule in the solid at low temperatures, e.g., two orientations of the μ_3-benzene relative to the basal Os_3 triangle that correspond to potential energy minima in the lattice.

If the barrier to interconversion between these states via torsional oscillation (libration) was sufficiently low, the mean atomic positions as determined in the room temperature X-ray diffraction experiment could represent the observed "symmetrically eclipsed" structure as a time-average of all possible atomic displacements and should be reflected in large msd parameters for the ring-carbon atoms about the pseudo-3-fold axis. In this case a crystallographic study at low temperatures should detect a positionally disordered ring if the C–C image pairs were sufficiently separated to be resolved. Alternatively, multiple olefin orientations could be invoked to account for this resonance multiplicity in the lattice. We see no evidence for irregularities among the thermal parameters for the ring or olefin carbons in **1**, but note that the large X-ray absorption corrections applied in the refinement of the structure could easily mask any low-amplitude librational motions. Moreover, the marked magnetic anisotropy associated with the metal–ligand interactions in this complex suggests that even small ligand displacements could lead to the observed chemical shift splittings. The coalescence of the C_6 and C_2 resonance "pairs" on warming from 230 to 250 K, prior to significant exchange-broadening into the remaining ring nuclei, seems consistent with these suggestions.

Spectra in the low field CO region are also markedly temperature dependent, but the averaging by the fluxional processes is rather different from the behavior seen in solution. At 230 K

---

(39) (a) Braga, D.; Heaton, B. T. *J. Chem. Soc., Chem. Commun.* **1987**, 608. (b) Anson, C. A.; Benfield, R. E.; Bott, A. W.; Johnson, B. F. G.; Braga, D.; Marseglia, E. A. *J. Chem. Soc., Chem. Commun.* **1988**, 889.

(40) The line widths in the organic ligand region are generally much larger than those in the carbonyl region and larger than expected for compounds of this type. Given that the experimental conditions were adjusted separately to give optimum resolution in each region of the spectrum it seems reasonable to assume that the linebroadening is due to effects promoted by motion of or within the cluster compound.

(41) For a system in which ^{13}C spins are dipolar coupled to ^1H spins experiencing an rf decoupling field of frequency ω_1, two ^{13}C NMR line-narrowing regions are predicted: in the short correlation limit, $\omega_1\tau_c \ll 1$, while in the long correlation limit $\omega_1\tau_c \gg 1$ obtains. Maximum broadening occurs at $\omega_1\tau_c \sim 1$.[42]

(42) Rothwell, W. P.; Waugh, J. S. *J. Chem. Phys.* **1981**, *74*, 2721.

(43) Suwelack, D.; Rothwell, W. P.; Waugh, J. S. *J. Chem. Phys.* **1980**, *73*, 2559.

(44) Fyfe, C. A. *Solid State NMR for Chemists*; CFC Press: Guelph, Ontario, 1983.

several sharp signals are observed superimposed on a very broad resonance. The line shapes of both the isotropic chemical shift centerband and the sideband manifold may be studied, and extraction of the CSA tensors from the intensity profiles of the sideband manifolds[45] shows the sharp resonances to have anisotropies consistent with static carbonyls.[46] The varying intensities may be explained, in part, by differential cross polarization properties of carbonyls in differing environments due to different dipolar coupling strengths to the proton spin bath.[47] The broad component narrows on warming and by 270 K begins to emerge as a sharpening resonance centered at 178 ppm. The other CO signals are somewhat broadened at this temperature, and this general broadening continues as the temperature is raised, reaching a maximum at ~330 K.[48] Within this broadening regime the 178 ppm line continues to sharpen, gaining intensity in the centerband but losing intensity in the sidebands. The resonances at 172.5, 174, and 185 ppm broaden more than those at 173 and 188 ppm and indeed appear to coalesce at around 330 K. Importantly, the spectrum at 310 K shows that the central peak at 178 ppm has only a small anisotropy indicating that the carbonyls it represents are motionally averaged, while the pair of resonances at 173 and 188 ppm still have anisotropies consistent with static carbonyls.

Making direct chemical shift comparisons with the ^{13}C solution NMR spectrum at 145 K (see Figure 5) and recalling the three distinct turnstile processes in solution, it appears that in the solid state at 230 K the X/X′ and Z/Z′/Z″ carbonyl sets are static but the Y/Y′/Y″ set is fluxional and gives rise to the broad resonance observed.[49] Rearrangement within the Y/Y′/Y″ set approaches the fast limit by 310 K on both the exchange-broadening and chemical shift anisotropy time scales. Estimating a coalescence temperature of 230 K (T_C = 192 K for the equivalent process in solution) sets an upper limit for the barrier to CO_Y interchange of $\Delta G^*_{230} < 44.4$ kJ mol^{-1}. A substantially greater activation barrier to turnstile exchange among the Z/Z′/Z″ set ($\Delta G^*_{330} > 66$ kJ mol^{-1}) contrasts the facile ligand exchange behavior in solution, which is incompletely suppressed even at 145 K. These values may be compared with activation barriers previously derived for tricarbonyl rotations in [M(CO)$_3$(η^6-C$_6$H$_5$Me)], M = Cr, Mo, of 65 and 70–75 kJ mol^{-1}, respectively.[36] Finally the resonances at 173 and 188 ppm that are characteristic of static CO ligands to 330 K are assigned to the X/X′ carbonyl set, showing that the trigonal twist pathway that exchanges ligands in the Os(CO)$_2$(C$_2$H$_4$) polytope is a prohibitively high energy process in the solid state.[50] This is consistent with the X-ray diffraction study which does *not* support disorder of the ethylene ligand between the two equatorial sites. Line shape simulations for the upfield organic ligand region of the ^{13}C{^{1}H} CP/MAS spectra from density matrix calculations in Liouville space[51] were performed using the program DNMR4.[52] These suggest Eyring activation energies of $\Delta G^* = 52.1–55.0$ kJ mol^{-1} for ethylene rotation (>41 kJ mol^{-1} in solution), $\Delta G^* = 49.8–53.8$ kJ mol^{-1} for 1,2 ring jumps ($\Delta G^*_{211} = 48.3 \pm 0.3$ kJ mol^{-1} in solution), and $\Delta G^* = 51.6–55.2$ kJ mol^{-1} for random jumps of the benzene ring over the temperature range studied, in reasonable agreement with the value of $\Delta G^*_{330} = 50.5$ kJ mol^{-1} found for both ligand rearrangements on the assumption of broadening from the "dipolar decoupling" regime.

In summary, of the five dynamic processes detected by NMR for **1** in solution, four prevail in the solid state. The ethylene ligand undergoes Cramer-type rotation about the Os–(C$_2$H$_4$) axis, and the crystallographic and ^{13}C CP/MAS studies together imply that the fluxional behavior of the face-capping benzene ligand is more accurately regarded as a ring "jumping" between discrete nuclear sites of minimum potential than as a hindered rotation where intermediate orientations might be populated for significant periods. The activation energies for these processes in the solid are little more than the values seen in solution and suggest that the barriers are principally due to electronic factors which are expected to be similar in solution and in the solid state.[53] It is not clear whether the similarity in activation energies for the two processes implies that the motions are positively correlated ("geared") in any way in the solid. Interchange within each of the Y/Y′/Y″ and Z/Z′/Z″ carbonyl ligand sets is observed, but with barriers that are significantly greater than for the equivalent rearrangements in solution. Moreover the relative ease of these rearrangements is reversed between the two phases, suggesting that intermolecular lattice interactions contribute less to energy barriers for "rigid body" motion (i.e., for the C$_6$H$_6$ and C$_2$H$_4$ rotors) than to carbonyl ligand exchange via a turnstile ligand interchange pathway. Packing effects in the solid are presumably sufficiently severe as to preclude olefin site-exchange between equatorial coordination sites.

Experimental Section

Methods and Materials. General experimental methods have been outlined in the preceding paper,[6a] and the μ_3-arene/olefin complexes [Os$_3$(CO)$_8$(η^2-CH$_2$CHR)(μ_3:η^2:η^2:η^2-C$_6$H$_6$)], R = H (**1**), Me (**2**), Ph (**3**), ^{t}*Bu* (**4**), were prepared as previously described.[6a]

Preparation of ^{13}CO Enriched [Os$_3$(CO)$_{12}$]. [Os$_3$(CO)$_{10}$(NCMe)$_2$][54] (500 mg) was placed in a 150-mL round-bottomed glass vessel with CH$_2$Cl$_2$ (50 mL), and the solution was subjected to several freeze–thaw–degas cycles. The evacuated vessel was then filled with ^{13}CO (1 atm), and the solution was stirred for 8 h at room temperature. A fine yellow precipitate of [Os$_3$(CO)$_{12}$] was filtered, and the filtrate was evaporated to dryness, giving quantitative conversion to ca. 15% ^{13}CO enriched [Os$_3$(CO)$_{12}$]. Repetition of the procedure with [Os$_3$(CO)$_{10}$(NCMe)$_2$] prepared from this enriched material gave [Os$_3$(CO)$_{12}$] with an approximate ^{13}CO enrichment level of 30%.

Preparation of ^{13}C-Labeled Cyclohexa-1,4-diene. Anhydrous liquid ammonia (50 mL) was condensed under an Ar atmosphere into a three-necked 100-mL flask equipped with a mechanical stirrer and a dry-ice/acetone condensor, which contained C$_5$C*H$_6$ (30% ^{13}C-enriched, M.S.D. Isotopes) (1.5 mL), THF (5 mL), and ^{t}*BuOH* (5 mL). Small pieces of sodium wire (2.0 g) were slowly added with constant, vigorous stirring, and the deep blue solution was maintained at −78 °C for 4 h. MeOH was carefully added to quench the reaction (until the blue coloration was completely discharged), and the vessel was removed from the dry-ice/acetone cooling bath to evaporate the ammonia. The residue was extracted with 2 × 20 mL portions of *n*-octane with the octane phase being washed thoroughly with water (five or more washings) before being dried over anhydrous MgSO$_4$. The octane solution of the labeled cyclohexa-1,4-diene was used directly in the preparation of [HOs$_3$(CO)$_9$(μ_3:η^2:η^1:η^2-C$_6$H$_7$)] as described in the following procedure. ^{1}H NMR indicated a benzene to diene conversion of better than 90% with isolated yields of approximately 25%.

Preparation of ^{13}C-Labeled [HOs$_3$(CO)$_9$(μ_3:η^2:η^1:η^2-C$_5$C*H$_7$)]. The octane solution of ^{13}C-labeled cyclohexa-1,4-diene, prepared as described above, and [H$_2$Os$_3$(CO)$_{10}$][55] (75 mg) were heated under reflux at 125

---

(45) (a) Maricq, M. M.; Waugh, J. S. *J. Chem. Phys.* **1979**, *70*, 3300. (b) Herzfeld, J.; Berger, A. E. *J. Chem. Phys.* **1980**, *73*, 6021. (c) Clayden, N. J.; Dobson, C. M.; Lian, L.-Y.; Smith, D. J. *J. Magn. Reson.* **1986**, *69*, 476.

(46) Gleeson, J. W.; Vaughan, R. W. *J. Chem. Phys.* **1983**, *78*, 5834.

(47) Yannoni, C. S. *Acc. Chem. Res.* **1982**, *15*, 201.

(48) This effect is again ascribed to benzene and olefin ligand motion on the time scale of the rf decoupling since it is to these protons that the carbonyl carbons are dipolar coupled.

(49) Very low intensity, but sharp, resonances seen at 170, 177, and 183 ppm occur at chemical shifts expected for a static Y/Y′/Y″ set by analogy with the solution spectrum. They have large anisotropies consistent with a static nature and remain relatively sharp until 285 K after which the general carbonyl broadening renders them unobservable. We suggest that they could be due to a minor crystalline form of **1** in which the Y/Y′/Y″ set is not fluxional.

(50) Accordingly, the only process which can average the alkene ^{13}C resonances in the solid state is Cramer-type rotation, and hence the benzene ligand resonances are not pairwise equilibrated by any ethylene site exchange prior to the jump-type benzene reorientation process, as in solution. This considerably simplifies the exchange pattern in the solid state, and the system is amenable to direct lineshape analysis.

(51) (a) Binsch, G. *Mol. Phys.* **1968**, *15*, 469. (b) Binsch, G. *J. Am. Chem. Soc.* **1969**, *91*, 1304.

(52) Bushweiler, C. H.; Letendre, L. J.; Brunelle, J. A.; Bilotsky, H. S.; Whalon, M. R.; Fleischman, S. H. *Quantum Chemistry Program Exchange*: Program No. 466, DNMR4.

(53) A wide-line ^{1}H NMR investigation of Fe$_2$(CO)$_5$(μ-C$_8$H$_8$) indicated that the planar C$_8$H$_8$ ring was fluxional in the solid, even at 77 K, corresponding to an activation barrier to rotation of ~8 kJ mol^{-1}.[34a]

(54) Johnson, B. F. G.; Lewis, J.; Pippard, D. A. *J. Chem. Soc., Dalton Trans.* **1981**, 407.

(55) Knox, S. A. R.; Koepke, J. W.; Andrews, M. A.; Kaesz, H. D. *J. Am. Chem. Soc.* **1975**, *97*, 3942.

°C for 2 h to give a yellow-orange solution. The solvent was carefully distilled off and reserved for a second reaction, the residue taken up in CH_2Cl_2 and separated by TLC, eluting with CH_2Cl_2 (30%)/hexane (70%). Extraction of a pale yellow band gave ^{13}C-labeled $[HOs_3(CO)_9(\mu_3:\eta^2:\eta^1:\eta^2\text{-}C_5C^*H_7)]$ in ca. 40% yield. The dienyl complex was converted to $[Os_3(CO)_9(\mu_3:\eta^2:\eta^2:\eta^2\text{-}C_5C^*H_6)]$ following the procedure described previously.[6a]

Solution NMR Experiments. Solution NMR spectra were obtained using a Bruker AM400 spectrometer operating at 400.1 MHz for ^1H and 100.6 MHz for ^{13}C. Samples were dissolved in CD_2Cl_2, and spectra were recorded in 5-mm tubes. For low temperature two-dimensional experiments samples were prepared at room temperature, cooled to ca. 200 K, and filtered to give saturated solutions (approximate concentrations of 55 and 32 mg mL^{-1} for the ethylene and styrene complexes, respectively). Temperature calibration was achieved with a methanol NMR thermometer using the method of van Geet.[56]

With the exception of the ^1H–^{13}C chemical shift correlation spectra, all two-dimensional spectra were recorded phase sensitively using the Marion–Wuthrich TPPI method,[27] and Lorentzian-to-Gaussian apodization was used in each dimension.

Acquisition Conditions. Double-Quantum-Filtered COSY.[57] t_1 was incremented in 256 steps to a maximum of 256/(2×SW1) s, and the data were zero filled to 512 words prior to Fourier transformation. Thirty-two scans per increment were recorded. Acquisition time in t_2 was 0.45 s giving 2048 real data points. Relaxation delay between experiments was 0.45 s.

Two-Dimensional CAMELSPIN.[15a] The mixing time consisted of a CW spin locking field of duration 0.2 s and field strength, $\gamma B_1/2\pi$, of 3.0 kHz. The same field strength was used for the remainder of the radio frequency pulses. t_1 was incremented in 256 steps to a maximum of 256/(2×SW1) s, and the data were zero filled to 512 words prior to Fourier transformation. Sixteen scans per increment were recorded. Acquisition time in t_2 was 0.2 s giving 2048 real data points. Relaxation delay between experiments was 0.6 s.

Two-Dimensional Exchange Spectra.[23] Carbon spectra were recorded using broadband proton decoupling (WALTZ-16).[58] t_1 was incremented in 256 steps to a maximum of 256/(2×SW1) s, and the data were zero filled to 512 words prior to Fourier transformation. Two hundred fifty-six scans were recorded for each increment. Acquisition time in t_2 was 0.51 s giving 4096 real data points. Relaxation delay between experiments was 0.25 s.

^1H–^{13}C Chemical Shift Correlation.[59] t_1 was incremented in 64 steps to a maximum of 64/SW1 s, and the data were zero filled to 128 words prior to Fourier transformation. Five hundred twelve scans were recorded per increment. Acquisiton time in t_2 was 0.21 s giving 2048 real data points. Relaxation delay was 1.0 s. An absolute value display was taken.

^1H and ^{13}C longitudinal relaxation times were recorded using an inversion-recovery sequence. Steady state NOE difference spectra were recorded in the usual way.[60]

Solid State NMR Experiments. ^{13}C CP/MAS NMR spectra were recorded at 50.32 MHz using a Bruker CXP200 spectrometer equipped with a multinuclear, proton-enhanced, double-bearing magic angle sample spinning probe, a high power proton decoupler, and an Aspect 2000 data system. A single contact spin-lock CP sequence with flip back of ^1H magnetization and with a proton rf field of 17 G was used.[61] Dry nitrogen was used for both spinning and bearing gases. Temperature regulation was of the bearing gas and temperature measurement was of the bearing exhaust close to the sample. Temperature calibration below room temperature was achieved with the samarium ethanoate tetrahydrate Curie law chemical shift thermometer previously calibrated against the phase transition of *d*-camphor[62] and above room temperature with the phase transitions of cobaltocenium hexafluorophosphate[63] and 1,4-diazabicyclo-[2,2,2]-octane.[62] The system was allowed to equilibrate at each new temperature for 1 h before spectral accumulation was commenced. The intensity of the ferrocene NMR resonance was measured at each temperature under otherwise identical conditions to provide a degree of temperature-dependent intensity calibration for the probe. Approximately 250 mg of a sample enriched to about 15% with ^{13}CO, together with a small amount of potassium bromide (the ^{79}Br resonance of which was used to set the magic angle[64] at each temperature), was packed into a 7-mm zirconia rotor with a Kel-F top. Typically 1000–2000 transients, with a relaxation delay of 3–15 s, were accumulated for each spectrum in the organic ligand region, and up to 600 transients, with a relaxation delay of 30–60 s, for the carbonyl region.

Acknowledgment. We thank Dr. K. G. Orrell, University of Exeter, for providing the two-dimensional EXSY analysis software, D2DNMR. M.A.G. gratefully acknowledges the financial support of the Royal Commission for the Exhibition of 1851 and the University Grants Committee (New Zealand).

Supplementary Material Available: Figures showing variable temperature ^1H and $^{13}C\{^1H\}$ NMR spectra for complexes **3** and **4**, ^1H two-dimensional CAMELSPIN spectrum of **3**, and $^{13}C\{^1H\}$ two-dimensional EXSY spectrum of **1** and a table of two-dimensional EXSY peak intensity data for **3** (8 pages). Ordering information is given on any current masthead page.

---

(56) Van Geet, A. L. *Anal. Chem.* **1970**, *42*, 679.

(57) (a) Piantini, V.; Sorensen, O. W.; Ernst, R. R. *J. Am. Chem. Soc.* **1982**, *104*, 6800. (b) Shaka, A. J.; Freeman, R. *J. Magn. Reson.* **1983**, *51*, 169.

(58) Shaka, A. J.; Keeler, J. *Prog. NMR Spectrosc.* **1987**, *19*, 47.

(59) Bax, A.; Morris, G. A. *J. Magn. Reson.* **1981**, *42*, 501.

(60) Sanders, J. K. M.; Mersh, J. D. *Prog. NMR Spectrosc.* **1982**, *15*, 353.

(61) (a) Pines, A.; Gibby, M. G.; Waugh, J. S. *J. Chem. Phys.* **1973**, *59*, 569. (b) Tegenfeld, J.; Haeberlen, U. *J. Magn. Reson.* **1986**, *69*, 191.

(62) Haw, J. F.; Campbell, G. C.; Crosby, R. C. *Anal. Chem.* **1986**, *58*, 3172.

(63) Heyes, S. J.; Clayden, N. J.; Dobson, C. M.; Wiseman, P. J., unpublished results.

(64) Frye, J. S.; Maciel, G. E. *J. Magn. Reson.* **1982**, *48*, 125.

Development and Mechanistic Study of a New Aldehyde Decarbonylation Catalyst

Faraj Abu-Hasanayn, Martin E. Goldman, and Alan S. Goldman*

Contribution from the Department of Chemistry, Rutgers, The State University of New Jersey, New Brunswick, New Jersey 08903. *Received December 11, 1990*

Abstract: $Rh_2(PMe_3)_2(CO)_2Cl_2$ (**2**) has been found to catalyze the decarbonylation of aldehydes to give the corresponding alkanes. Reaction rates are comparable to those of the most active nonradical systems previously reported. A mechanistic study indicates that the turnover-limiting reaction step includes addition of the aldehydic C–H bond to an intact molecule of **2**; ligand dissociation or cleavage of the chloride bridge does not occur prior to the C–H addition step. This conclusion is based on kinetic studies ($d[R'H]/dt = k_{obs}[\mathbf{2}][R'CHO]$; $R' = n\text{-}C_{11}H_{23}$; $k_{obs} = 2.2 \times 10^{-4}\ M^{-1}\ s^{-1}$; $\Delta S^* = -26$ eu) and the observation of a significant kinetic isotope effect ($k_{RCHO/RCDO} > 1.8$).

Our interest in the catalytic carbonylation of hydrocarbons has led us to consider the development of catalysts for the reverse reaction. In addition to its obvious relevance to alkane carbonylation, the decarbonylation of aldehydes is a useful and im-

0002-7863/92/1514-2520$03.00/0